

The 2-10 keV emission properties of PSR B1937+21

L. Nicastro¹, G. Cusumano¹, L. Kuiper³, W. Becker², W. Hermsen³, and M. Kramer⁴

¹ IASF-CNR, Via U. La Malfa 153, 90146 Palermo, Italy

² Max-Planck-Institut für extraterrestrische Physik, Giessenbachstraße, 85740 Garching, Germany

³ SRON National Institute for Space Research, Sorbonnelaan 2, 3584 CA Utrecht, The Netherlands

⁴ University of Manchester, Jodrell Bank, Macclesfield SK11 9DL, United Kingdom

Abstract. We present the results of a *BeppoSAX* observation of the fastest pulsar known: PSR B1937+21. The ~ 200 ks observation (78.5 (34) ks MECS (LECS) exposure times) allowed us to investigate with high statistical significance both the spectral properties and the pulse profile shape. The absorbed power law spectral model gave a photon index of ~ 1.7 and $N_{\text{H}} \sim 2.3 \times 10^{22} \text{ cm}^{-2}$. These values explain both *a.* the ROSAT non-detection and *b.* the deviant estimate of a photon index of ~ 0.8 obtained by ASCA. The pulse profile appears, for the first time, clearly double peaked with the main component much stronger than the other. The statistical significance is 10σ (main peak) and 5σ (secondary peak). The 1.6–10 keV pulsed fraction is consistent with 100%; only in the 1.6–4 keV band there is a $\sim 2\sigma$ indication for a DC component. The secondary peak is detected significantly only for energies above $3 \div 4$ keV. The unabsorbed (2–10 keV) flux is $F_{2-10} = 3.7 \times 10^{-13} \text{ erg cm}^{-2} \text{ s}^{-1}$, implying a luminosity of $L_X = 4.6 \times 10^{31} \Theta (d/3.6 \text{ kpc})^2 \text{ erg s}^{-1}$ and an X-ray efficiency of $\eta = 4 \times 10^{-5} \Theta$, where Θ is the solid angle spanned by the emission beam. These results are in agreement with those obtained by ASCA.

PSR B1937+21, with a period $P = 1.56$ ms, was the first and still the fastest MSP known. In spite of its low surface magnetic field strength of $B_S = 4.1 \times 10^8$ G, its magnetic field at the light-cylinder is the highest of all known pulsars: $B_L \simeq 1 \times 10^6$ G, very similar to that of the Crab pulsar. Its spin-down flux density is $\sim 2 \times 10^{-10} \text{ erg cm}^{-2} \text{ s}^{-1}$, which is 3 times higher than for PSR J0218+4232 but 3 times lower than for PSR B1821–24.

Here we report on the results obtained by a *BeppoSAX* observation in the energy range 1.6–10 keV.

2. Observation and spatial analysis

BeppoSAX observed PSR B1937+21 on May 1st 2001. The ~ 200 ks observation time resulted in a total effective on-source time of ~ 78.5 ks (~ 34 ks) with the MECS (LECS). To extract the source photons from LECS (0.1–10 keV) and MECS (1.6–10 keV), we used:

- a standard spatial analysis with optimized extraction radius and energy range;
- a Maximum Likelihood (ML) approach to extract the number of counts assigned to the pulsar taking into account the presence of other sources and the background simultaneously.

1. Introduction

The various X-ray satellites, from Rosat to Chandra, observed about 10 millisecond pulsars (MSPs) (see e.g. Becker 2001), but good spectral and temporal informations exist only for half of them. In fact MSP X-ray observations are usually affected not only by low statistics but also by insufficient time accuracies to perform detailed periodicity and timing analysis. X-ray observations demonstrate that the X-ray emission from MSPs is generally not of thermal origin, and those with the hardest spectra appear to be objects with strong magnetic fields at the light-cylinder B_L ($R_L = cP/2\pi$; see Saito et al. 1997, Kuiper et al. 1998, Kuiper et al. 2000, Becker 2001). Given the correlation between spin-down power and X-ray luminosity (see Verbunt et al. 1996, Becker and Trümper 1997 and Takahashi et al. 2001), another important quantity is the spin-down flux density at Earth ($E/4\pi d^2$).

In the first case we estimated the local background (in a circular region in the field of view $10'$ away from the pulsar) and compared the results with the standard one from archival blank sky usually used in the spectral fitting. We found that the local background is 50% and 15% higher for LECS and MECS respectively. The extraction radii which optimized the signal to noise ratio were $3'$ (LECS) and $2'$ (MECS) resulting in a collection of 106 (0.5–8 keV) and 369 (1.6–10 keV) photons. In spite of the lower exposure time and sensitivity of LECS we were able to detect a significant signal in the 0.5–8 keV range for this instrument. Inclusion of these softer photons in the spectral fit allowed us to better constrain the hydrogen column density toward the pulsar (N_{H}). Using the ML approach we could extract the source photons modeling the contribution to the total counts from additional field sources and

the (assumed flat) background. This method was successfully used in several other cases of weak source (see e.g. Kuiper et al. 1998, Mineo et al. 2000).

3. Temporal analysis

The arrival times of the extracted photons were converted to the Solar System Barycentric (SSB) Frame using the BARYCONV¹ code and then searched for periodicities by folding them with trial frequencies around the radio one (see updated radio ephemeris in Table 1). The χ^2 value plotted versus trial frequency is shown in Fig. 1. The distribution had a clear maximum, but we found the corresponding pulse frequency deviating from the radio value by $\simeq -7.6 \times 10^{-6}$ Hz ($f_R - f_X$). This is about ten times the statistical error of $\sim 8 \times 10^{-7}$ Hz. To investigate this discrepancy we first verified the correctness of the SSB conversion code by also using independent software. We verified that all the routines involved in the processing were working properly. We then verified the OBT (On-Board Time) to UTC time conversion routine. To this aim we:

1. analyzed separately two sections of the observation; the results confirmed those of the full observation;
2. used different polynomial order for the OBT–UTC fit and various high deviation points (de-)selection criteria; in all cases the results were the same;
3. verified the (X-ray) pulse frequency of the Crab during the observation performed on April 2000 and on September 2001; these observations are shorter than the PSR B1937+21 one (in particular the 2001 observation), nevertheless in the first case we found a discrepancy which is outside the statistical errors.

We concluded that the difference had likely to be attributed to incorrect photon time markers. We investigated the possible reasons of that with the *BeppoSAX* mission director. The answer was that, excluding an unlikely (and unobserved) UTC clock drift (which comes out of the Malindi ground station GPS clock), the only likely explanation could be an on-board electronics problem. In particular it could be an internal drift of the clock which tags the “base band” packets. Performance degradation with time of the clock is not unexpected and usually not considered critical for detectors not specifically built for high precision timing. Also, as we verified with the Crab, the problem is less severe (or not visible) for pulsar with relatively long periods or for relatively short observations. Even though other (we believe more unlikely) explanations could be found, we decided to correct the (possible) clock drift by estimating the required additional slope to add in the OBT–UTC conversion. The result was a constant slope of $\sim 1 \times 10^{-8}$ s s⁻¹. We verified this value (actually a value slightly lower) could also correct the 2000 Crab

Table 1. Ephemeris of PSR B1937+21 (from observations performed at Effelsberg).

Parameter	Value
Right Ascension (J2000)	19 ^h 39 ^m 38 ^s .560
Declination (J2000)	21° 34′ 59″.14
Epoch validity start/end (MJD)	51639 – 52047
Frequency	641.928246349481 Hz
Frequency derivative	-4.331×10^{-14} Hz s ⁻¹
Epoch of the period (MJD)	51843.0
RA proper motion	-0.15 mas yr ⁻¹
Dec proper motion	-0.47 mas yr ⁻¹

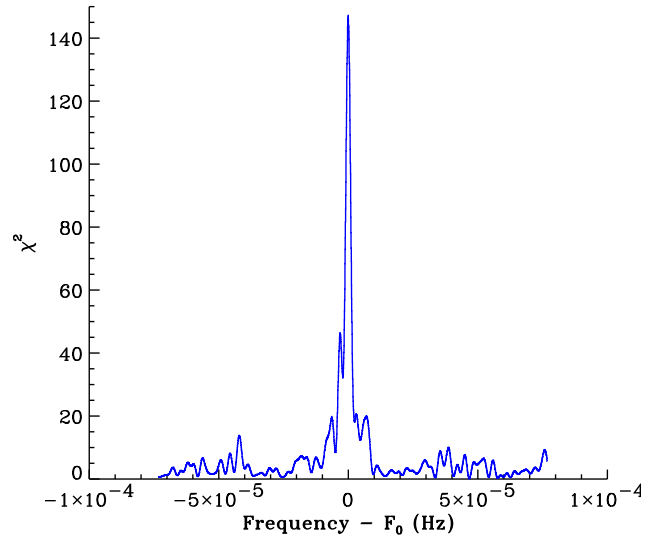


Fig. 1. The χ^2 significance as function of trial folding frequency. The 0 is aligned with the maximum.

observation (~ 70 ks elapsed time) while it had no effect on the 2001 observation (~ 24 ks elapsed time).

Counting statistics allowed us to perform temporal analysis only for the MECS data (actually a search on the LECS photons didn’t reveal any significant modulation). As already mentioned, a periodicity search analysis was performed on the 369 photons (1.6–10 keV) around the nominal radio period, after converting the arrival times to the SSB. Figure 2 shows the folded light curve together with the radio one (from the EPN archive² – Kramer et al. 1998). The primary peak (P1) is detected at 10σ level and, for the first time, we also detect the secondary peak (P2 – significance $\sim 5\sigma$) and estimate a relative phase separation of 0.48 ± 0.04 . Data collected by ASCA allowed Takahashi et al. (2001) to claim an alignment of the main X-ray peak with the radio interpulse. We then arbitrarily aligned the two profiles (the BSAX on-board clock absolute calibration does not allow to do it for a

¹ see <http://www.sdc.asi.it/software/saxdas/baryconv.html>

² see <http://www.mpifr-bonn.mpg.de/pulsar/dat/>

Table 2. Power law fit parameters using photons extracted with the standard and the Maximum Likelihood methods.

Method	K^a	α	N_{H} (10^{22} cm^{-2})	F_{2-10}^b
STD	0.85	$1.66^{+0.07}_{-0.06}$	$2.27^{+0.58}_{-0.47}$	3.7 ± 0.4
ML	$1.12^{+0.10}_{-0.10}$	$1.71^{+0.06}_{-0.08}$	$2.10^{+0.56}_{-0.42}$	3.7 ± 0.4

Note: all quoted uncertainties are 1σ confidence. It is $N_{ph}(E) = K \times E^{-\alpha}$.

^a Normalization at 1 keV ($10^4 \text{ ph s}^{-1} \text{ cm}^{-2}$).

^b Unabsorbed flux in 2–10 keV ($10^{-13} \text{ erg cm}^{-2} \text{ s}^{-1}$).

MSP). The vertical dashed lines in the figure are exactly 0.5 apart. The radio peaks separation is instead 0.4794(8) so it would be tempting to consider the ASCA result incorrect and consider P1 be coincident with the main radio peak. The X-ray peak widths are compatible with the instrument time resolution limit ($\sim 100 \mu\text{s}$). Figure 3 shows the X-ray pulse profile in 3 energy ranges. In an attempt to quantify the evidence for a pulsar DC component, we applied the bootstrap method proposed by Swanepoel et al. (1996), which allows us to estimate the DC level (sky background and possibly a source component) in the pulse profile. We can then determine the DC and pulsed fractions of the pulsar by taking the background level from the spatial analysis into account. However, in the available form, the bootstrap method is able to find only one unpulsed interval and cannot account for systematic errors. One should therefore realize that the quoted errors on the calculated parameters are only statistical. Note in Fig. 3 how the DC level is compatible with the background level. We find that over the total energy range 1.6–10 keV the source is consistent with being 100% pulsed; the 2σ lower limits for the pulsed fraction in the energy ranges 1.6–10, 1.6–4 and 4–10 keV are 88%, 66% and 95%, respectively. Only for the lower 1.6–4 keV energy interval we find an indication for a DC component of $(18.7 \pm 7.7)\%$. An increase of P2 compared to P1 with energy is clearly visible.

4. Spectral analysis

The spectral analysis was performed using photons extracted in two different ways: *a.* those in a (S/N optimized) circular region centered on the pulsar position (standard method); *b.* those from the ML analysis, which consider simultaneously the source, the background and a number of field sources. In both cases the best fitting model was an absorbed power law. A Black Body model did not fit the data satisfactorily. The two methods gave consistent results and are summarized in Tab. 2. The absorbed flux (2–10 keV) is $3.1 \times 10^{-13} \text{ erg cm}^{-2} \text{ s}^{-1}$.

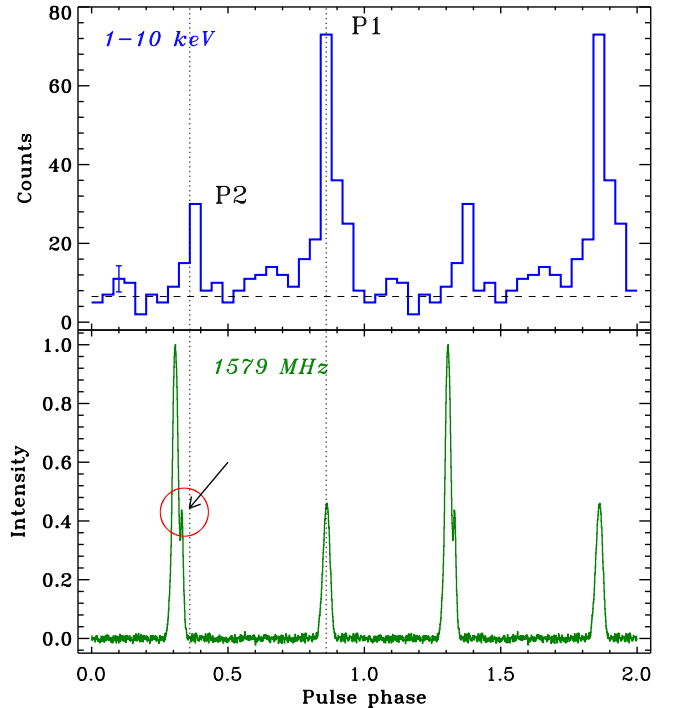


Fig. 2. The 1.6–10 keV X-ray profile and the radio one arbitrarily aligned using the main X-ray peak. The two vertical dotted lines are 0.5 apart. The X-ray phase separation is 0.48 like for the radio but 0.5 shifted in phase (if the ASCA result is correct). In this case we can also confidently exclude that the secondary X-ray peak is associated with the feature visible in the main radio peak (which instead would mimic the X-ray feature in P1).

The derived (unabsorbed) luminosity is $L_X = 4.6 \times 10^{31} \Theta (d/3.6 \text{ kpc})^2 \text{ erg s}^{-1}$ while the X-ray conversion efficiency is $\eta = L_X/E = 4 \times 10^{-5} \Theta$, where Θ is the solid angle spanned by the emission beam. Note that the column density is 10 times greater than the radio DM derived one (by assuming 10 H atoms for each e^-) and is only marginally consistent (within 2σ) with the Galactic value $1.4 \times 10^{22} \text{ cm}^{-2}$. In addition the photon index is significantly softer than that found for PSR J0218+4232 (0.94 ± 0.22) and PSR B1821–24 (~ 1.1 using RXTE data, Kawai and Saito 1999). Also for the latter pulsar (placed in the globular cluster M28, at a distance of $\sim 5 \text{ kpc}$, galactic latitude $-5^\circ 6'$) its $N_{\text{H}} \simeq 3 \times 10^{21} \text{ cm}^{-2}$, consistent both with the Galactic and DM derived one. Being the line of sight to PSR B1937+21 tangent to the Galactic spiral arms ($l \simeq 57.51$, $b \simeq -0.29$, see Taylor and Cordes 1993) one can invoke a particularly low e^-/N_{H} ratio in that direction due to the lack of ionizing sources. However, using the relation $N_{\text{H}} = 1.79 \times 10^{21} A_V$ of Predehl and Schmitt (1995), Verbunt et al. (1996) set an upper limit of $2.2 \times 10^{21} \text{ cm}^{-2}$ for the column density, i.e. in agreement with the DM value. More simply, the mea-

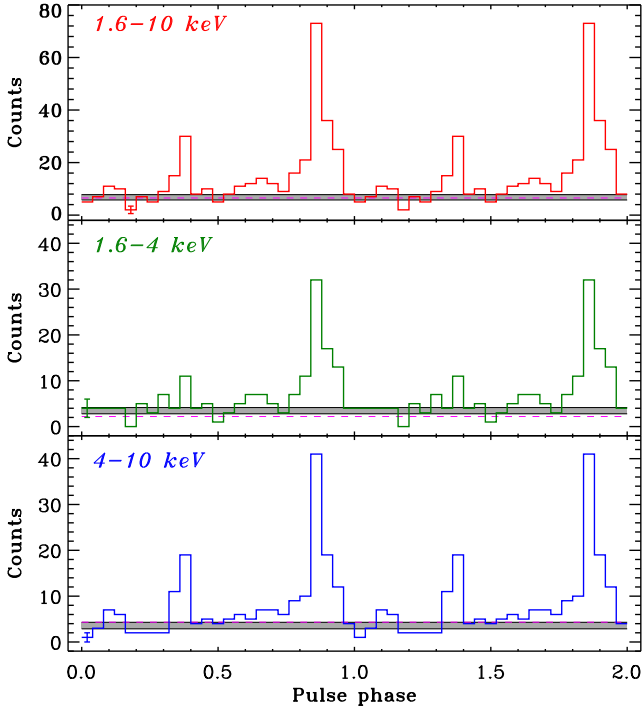


Fig. 3. The X-ray pulse profile in the full MECS X-ray band 1.6–10 keV and two sub-bands. The shaded areas show the estimated DC level ($\pm 1\sigma$), while the dashed lines indicate the measured background level. In the 1.6–4 keV energy band the secondary peak is detected at $\lesssim 3\sigma$ level and is compatible with the DC level. In the 4–10 keV band instead the detection level is 4σ (above background or DC level).

sured high N_{H} could suggest for PSR B1937+21 a true distance greater than the 3.6 kpc derived from the Taylor and Cordes (1993) model. If instead this value is correct then the continuing radio timing measurements should be able to detect its effect on the timing fit residuals very soon. We also note that the fit parameters are consistent with the non-detection in the ROSAT HRI energy range (0.1–2.4 keV).

5. Conclusions

We detected the double peak profile of the fastest pulsar known. The 1.6–10 keV pulsed fraction is consistent with 100%, only for the band 1.6–4 keV there is an indication for a DC component ($18.7 \pm 7.7\%$). The secondary (X-ray) peak is significantly detected only above 3–4 keV and the ratio primary/secondary decreases with energy. It was not possible to perform an absolute phase comparison with the radio profile, but, *purely* morphologically, a phase separation comparison suggests alignment of the main X-ray peak with the main radio one, contrary to the ASCA finding by Takahashi et al (2001) which claim an align-

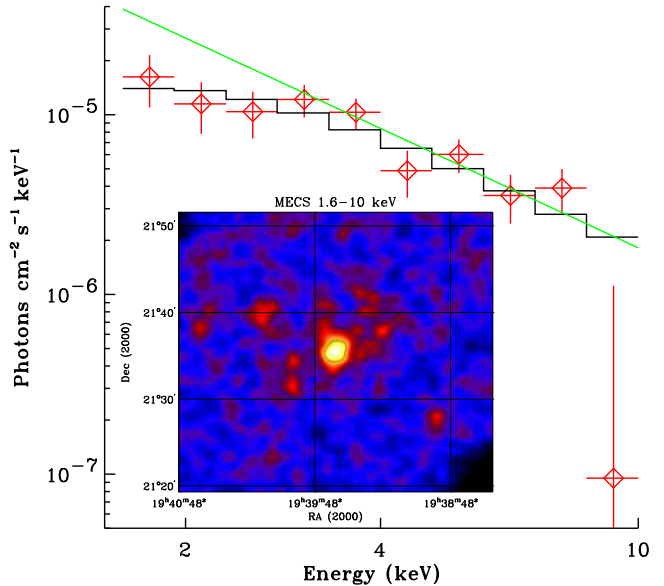


Fig. 4. The 1.6–10 keV spectrum and best fit model with the unabsorbed power law ($\alpha = 1.66$). It is evident the strong absorption below ~ 3 keV. In the inset the smoothed MECS image around the PSR position is shown.

ment with the radio interpulse. An accepted Rossi-XTE observation will clarify this point.

We measure a soft power law spectral index ($\alpha \simeq 1.7$), different from those measured for PSR J0218+4232 and PSR B1821–24. The $N_{\text{H}} \sim 2.3 \times 10^{22} \text{ cm}^{-2}$ is marginally consistent with the Galactic value in the direction of the pulsar and gives a e^-/N_{H} ratio of 1/100, 10 times smaller than the canonical average value. This could be justified by the position of PSR B1937+21 in the Galaxy w.r.t. our line of sight but could also suggest a larger distance than the DM derived one. Radio timing should settle this issue soon.

Acknowledgements. This research is supported by the Italian Space Agency (ASI) and Consiglio Nazionale delle Ricerche (CNR). BeppoSAX is a major program of ASI with participation of the Netherlands Agency for Aerospace Programs (NIVR).

References

- Becker W., Trümper J., 1997, A&A 326, 682
- Becker W., 2001, in *X-ray Astronomy '99: Stellar Endpoints, AGN & the Diffuse X-ray Background*, eds N. White et al., AIP Conference Proceedings 599, p. 13-24
- Kawai N., Saito Y., 1999, Proc. 3rd INTEGRAL Workshop, Taormina, Astroph. Lett. & Comm. Vol. 38, I, p.1.
- Kramer M., et al., 1998, ApJ 501, 270
- Kuiper L., Hermsen W., Verbunt F., Belloni T., 1998, A&A 336, 545
- Kuiper L., Hermsen W., Verbunt F., et al. 2000, A&A 359, 615

- Mineo T., Cusumano G., Kuiper L., et al., 2000, *A&A* 355, 1053
Predehl P., Schmitt J., 1995, *A&A* 293, 889
Takahashi M., Shibata S., Torii K., et al., 2001, *ApJ* 554, 316
Saito Y., Kawai N., Kamae T., et al., 1997, *ApJ* 477, L37
Swanepoel J.W.H., de Beer C.F., Loots H., 1996, *ApJ* 467, 261
Taylor J.H., Cordes J.M., 1993, *ApJ* 411, 674
Verbunt F., Kuiper L., Belloni T., et al., 1996, *A&A* 311, L9